

MODELLING OF BRITTLE ZONES IN THE HAZ OF STEEL WELDS

S. Suzuki, G.I. Rees and H. K. D. H. Bhadeshia †

ABSTRACT

A model is presented which allows the calculation of the fraction of hard phase as a function of the alloy chemistry, austenite grain size and the cooling rate. The results are used to obtain some general indications on the propensity of alloys to develop "local brittle zones" in the heat affected regions of welded plate, and to explain some trends in experimental observations.

INTRODUCTION

Local brittle zones (LBZ's) are small regions of hard brittle phase (usually martensite) which form in the heat affected zones (HAZ's) of multipass welds (Ref. 1). In experiments where the toughness of the HAZ is measured, the presence of minute brittle regions causes scatter in the measured data, because if the test specimen samples a brittle zone then the toughness is very low (Ref. 2). Scatter in mechanical property data is not only disconcerting, but also makes design difficult because of the existence of a few very poor values.

Experimental data have been interpreted to conclude that the lower bound toughness values deteriorate as the volume fraction of hard phase in the form of LBZ's increases (Ref. 3). However, the same data can be assessed to indicate that there is a minimum in the toughness as a function of increasing fraction of martensite. The purpose of this work was to begin addressing the problem of microstructural development in the HAZ using thermodynamic and kinetic phase transformation models, and to see whether interesting comments can be made about the development of LBZ's. We concentrate primarily on martensite as the culprit phase in LBZ's.

COOLING CURVES

Ashby and Easterling (Ref. 4) have shown that for the heat affected zone which is well away from the welding arc, the Rosenthal equations can be adapted and represented as a product of two functions:

$$T - T_0 = \frac{\phi_1 \Delta t}{t} \exp \left\{ -\frac{\Delta t \phi_1}{c (T_p - T_0) t} \right\} \quad (1)$$

† Cambridge University/JRDC, Dept. of Materials Science and Metallurgy, Pembroke Street, Cambridge CB2 3QZ, U.K.

where T_0 is the preheat temperature, T_p is the peak temperature of the thermal cycle and Δt is the cooling time between 800 °C and 500 °C

$$\Delta t = \frac{q/v}{2\pi\lambda} \left(\frac{1}{500 - T_0} - \frac{1}{800 - T_0} \right) \quad \text{and} \quad \frac{1}{\phi_1} = \left(\frac{1}{500 - T_0} - \frac{1}{800 - T_0} \right)$$

where q is the arc power, v is the arc speed and λ is the thermal conductivity. Since, during cooling through the temperature range 800 °C to 500 °C the cooling rate is not strongly dependent on T_p (Ref. 5) we can characterise the cooling of the welding cycle in terms of the characteristic time Δt in a similar manner to which a linear cycle can be described by the cooling rate.

TRANSFORMATION KINETICS OF ALLOTRIOMORPHIC FERRITE

It is assumed that the growth of this phase occurs with local paraequilibrium at the interface, with the rate being controlled by the diffusion of carbon in the austenite ahead of the interface. Transformation is also assumed to begin with an infinitesimally thin when the Scheil rule is satisfied for the C-curve of the TTT diagram for allotriomorphic ferrite. There is, at the transformation start temperature, a uniform layer of allotriomorphic ferrite at all of the austenite grain surfaces. For continuous cooling transformation it is assumed that the kinetics are additive with temperature. In the context of transformation from partially reaustenitised material, the approximation that all austenite boundaries are decorated with ferrite is reasonable, since ferrite can grow directly from that which remains after heating.

Growth of allotriomorphic ferrite is allowed to continue until another phase is able to nucleate and grow (*e.g.* Widmanstätten ferrite or bainite) which has a kinetic advantage over the allotriomorphic ferrite. If the nucleation of bainite or Widmanstätten ferrite is impossible, then the allotriomorphic ferrite growth is allowed to continue until martensite can form, despite the fact that the growth rate will decrease dramatically with temperature, as the diffusivity of carbon decreases.

For slow cooling rates, for which the extent of transformation to allotriomorphic ferrite will be very large, it is likely that pearlite formation will follow the allotriomorphic ferrite reaction. It is eventually hoped to incorporate a model for this transformation into the present work (Ref. 6).

GROWTH KINETICS OF WIDMANSTÄTTEN FERRITE

The lengthening rate of Widmanstätten ferrite plates has been shown (Ref. 7) to be well described by Trivedi's model for the diffusion controlled growth of parabolic cylinders, in which the curvature of the transformation interface modifies the local equilibrium at the plate tip. The application of this theory to weld metal transformation requires the incorporation of a limiting time in which growth can occur before impingement with intragranular nucleated phases brings transformation to an end. In the heat affected zone of welds, such

intragranular nucleation is not expected to occur (unless the steel has been deliberately inoculated). It is therefore necessary to modify the treatment applied earlier (Ref. 8), with the added condition that the nucleation of this phase has a gestation period.

This is easily done using a model (Ref. 9) for estimating the TTT curves of low-alloy steels. The lower C-curve of such diagrams represents the initiation of displacive transformations (Ref. 9). At a given temperature T_i the time required to initiate transformation is τ_i . Under continuous cooling conditions we use the Scheil approximation, whereby nucleation is assumed to have occurred when

$$\sum_i \frac{\Delta t_i}{\tau_i} = 1$$

where Δt_i represents the duration of the time spend at temperature T_i when the cooling curve is represented by a series of short isothermal holds. The summation applies only to the lower C-curve in the case of Widmanstätten ferrite nucleation. If by the time it is possible to nucleate Widmanstätten ferrite the thermodynamic conditions for the formation of bainite are satisfied (Ref. 9) then the nucleus is assumed to develop into bainite, since it has been shown (Ref. 9) that the requirement for nucleation of these two phases is expressed by the same function of temperature.

In order to determine the overall transformation kinetics of Widmanstätten ferrite it is necessary to take account of the surface area available for nucleation. The assumptions made concerning the nature and geometry of the available surface are as follows. Ferrite/austenite and austenite/austenite interfaces are assumed to be equally suitable as nucleation sites. The morphology of the austenite grains is assumed to be that of a truncated regular octahedron (tetrakaidecahedron).

From stereological considerations, for a tetrakaidecahedron of edge length b the volume of the grain V and the surface area per unit volume of the grain S_v are related to b by

$$V \propto b^3 \quad S_v \propto 1/b$$

when a fraction f_α of the grain has transformed to ferrite, the volume and surface area of the austenite are modified so that the new surface area of austenite per unit volume S'_v becomes

$$S'_v = S_v(1 - f_\alpha)^{2/3} \quad \text{i.e.} \quad S'_v = \frac{2(1 - f_\alpha)^{2/3}}{\bar{L}}$$

where \bar{L} is the mean linear intercept of the original austenite grain structure after reaustenitisation.

If it is assumed that the temperature interval in which Widmanstätten ferrite can form is small, *i.e.* temperatures at which nucleation by a displacive mechanism is possible, but the growth of bainite is impossible, then we can consider the nucleation rate of Widmanstätten

ferrite to be constant. An approximate expression for the overall transformation kinetics of the phase then becomes (Refs. 6, 10)

$$V_w = v_m \left(1 - \exp \left\{ - \frac{S'_v G_w f_1 \{T, t, x\} t}{v_m} \right\} \right)$$

where v_m represents the limiting volume fraction of Widmanstätten ferrite given when the austenite carbon composition reaches the paraequilibrium Ae'_3 value. With f_1 equal to a constant, this expression in effect assumes that the sideways impingement of plates occurs very rapidly within Widmanstätten ferrite packets, so that the growth kinetics are controlled mainly lengthening rate of plates. It is assumed that $f_1 = 0.5$ on the grounds that only half the available surface is correctly oriented to stimulate nucleation of either Widmanstätten ferrite or bainite.

GROWTH KINETICS OF BAINITE

The conditions for the nucleation of bainite are identical to those expressed in the previous section for Widmanstätten ferrite provided that the driving force for diffusionless growth is greater than 400 J mol^{-1} (Ref. 9). This is satisfied at the austenite composition $x_{T'_0}$ (Ref. 9). At a given temperature T_i a limit to the extent of transformation therefore exists, when the untransformed austenite carbon content reaches $x_{T'_0}$. This limiting volume fraction is denoted by θ , where

$$\theta = (x_{T'_0} - x^\gamma) / (x_{T'_0} - x^{\alpha'})$$

The growth of bainite plates occurs much faster than that calculated assuming carbon-diffusion control, but bainite forms in collections of plates called *sheaves*. These sheaves lengthen at a rate which is only slightly larger than carbon-diffusion control (Ref. 9). Since the key interest here is overall transformation kinetics, we assume that G_b , the lengthening rate of bainite sheaves is indeed carbon diffusion controlled. V_b , the overall fraction of the untransformed austenite that transforms to bainite, is then given by

$$V_b = \theta \left(1 - \exp \left\{ - \frac{S'_v G_b f_2 t}{\theta} \right\} \right)$$

where $f_2 = 0.5$ as discussed for Widmanstätten ferrite.

RESULTS AND DISCUSSION

In the context of local brittle zones, martensitic regions should only be detrimental if the carbon concentration is high. Prior to martensitic transformation, the austenite is enriched by the partitioning of carbon as other forms of ferrite grow. Consequently, a large fraction of ferrite prior to martensite formation is a necessary condition for the occurrence of LBZ's, otherwise the degree of carbon enrichment will be insufficient to render the martensite brittle. To permit comparisons, we arbitrarily fix the fraction of transformation that has to occur above the martensite start temperature to be 0.9, in

order for the subsequent martensite to be classified as a LBZ. A number of variables have been studied: the austenite grain size, alloy chemistry (C, Mn, Si), cooling time ($\Delta t_{800-500}$) and partial reaustenitisation during the heating cycles. This latter case is dealt with by assuming that only half the microstructure becomes austenitic during heating, and that the allotriomorphic ferrite simply grows off the existing ferrite.

Fig. 1a shows the results for a plain carbon steel (Fe-0.1C wt.%) with an austenite grain size (mean lineal intercept) of $100 \mu\text{m}$ - the white regions in the plots represent martensite. As expected, the amount of martensite that forms increases with cooling rate, but the carbon concentration of that martensite decreases at the same time. Hence, LBZ formation is actually more likely when the cooling rate is low (the cooling time large).

The effect of partial austenitisation during heating is illustrated in Fig. 1b, which shows that LBZ formation is promoted by the fact that the total amount of ferrite present is larger, leading to a higher carbon and lower volume fraction of martensite. Consequently, LBZ's are more likely in regions which experience multiple thermal cycles within the austenite formation range.

Fig. 1c shows that a reduction in the austenite grain size to $30 \mu\text{m}$ makes the situation worse in that the carbon concentration of the martensite is increased (its volume fraction reduced). This is because a smaller austenite grain size allows more transformation to occur before martensite.

The effect of adding an austenite stabilising element is illustrated in Fig. 2a which represents calculations for an Fe-1Mn-0.1C wt.% steel with a $100 \mu\text{m}$ austenite grain size. Comparison with Fig. 1a shows that the propensity to form LBZ's is reduced since the hardenability of the steel is improved. On the other hand, the addition of silicon (which accelerates the formation of ferrite) tends to make the situation slightly worse with respect to LBZ formation, as can be seen by comparing Fig. 2b and Fig. 1a.

The differences between the plain carbon and alloy steels are not so prominent, as far as LBZ formation is concerned, when the austenite grain size is reduced (compare Figs. 3a, 3b with Fig. 1c).

Finally, it should be emphasised that the comparisons made here are qualitative, since the model does not as yet include the formation of pearlite, although it could be argued that both pearlite and martensite are hard phases which form LBZ's. In addition, the theory employed is crude in its consideration of overall transformation kinetics, so that the work needs to be developed much further before quantitative comparisons can be made. The problem of austenite formation during the heating cycle has been bypassed as discussed in the text, whereas a full model requires also a treatment of austenite formation kinetics.

CONCLUSIONS

A model has been developed which is capable of correctly reflecting the trends of microstructure development that are observed during continuous cooling transformation. The work provides a basis for extension of existing phase transformation models for fusion zone microstructures to those which form in the heat affected zone. Further work is necessary before quantitative predictions can be made with confidence.

ACKNOWLEDGMENTS

The authors are grateful to Professor C. J. Humphreys for the provision of laboratory facilities. The work has been sponsored by NKK Japan, and via the "Atomic Arrangements: Design and Control Project", which is a collaborative effort between the University of Cambridge and the Research and Development Corporation of Japan.

REFERENCES

1. Fairchild, D. P. 1987. Local Brittle Zones in Structural Welds. Welding Metallurgy of Structural Steels, ed. J. Y. Koo, TMS-AIME, Warrendale, PA 303-318.
2. Schwalbe, K.-H; and Koçak, M. 1992. Fracture Mechanics of Weldments, Problems and Progress for Weldments. International Trends in Welding Science and Technology, eds. S. A. David and J. M. Vitek, ASM International, USA 479-494.
3. Aihara, S.; and Okamoto, K. 1990. Influence of LBZ on HAZ toughness of TMCP steel. Metallurgy, Welding and Qualification of Microalloyed Steel Weldments, eds. J. T. Hickey, D. G. Howden and M. D. Randall, AWS, Florida. 402-427.
4. Ashby, M.F.; and Easterling, K.E. 1969. Acta Metallurgica 30 1982
5. Reed, R.C. 1990. Ph.D. Thesis, University of Cambridge, U.K.
6. Umemoto, M. and co-workers 1992. I.S.I.J. Int. 32 306-315.
7. Bhadeshia, H.K.D.H. 1985. Mat. Sci. & Tech. 1 497-504.
8. Bhadeshia, H. K. D. H.; and Svensson, L.-E. 1993. Mathematical Modelling of Weld Phenomena, eds. Cerjak and Easterling, Institute of Materials, London, U.K. 109-182.
9. Bhadeshia, H. K. D. H. 1992. Bainite in Steels, Institute of Materials, London, U.K.
10. Christian J.W. 1975. Theory of Transformations in Metals and Alloys, Part I, 2nd edition, Pergamon Press, Oxford, U.K.

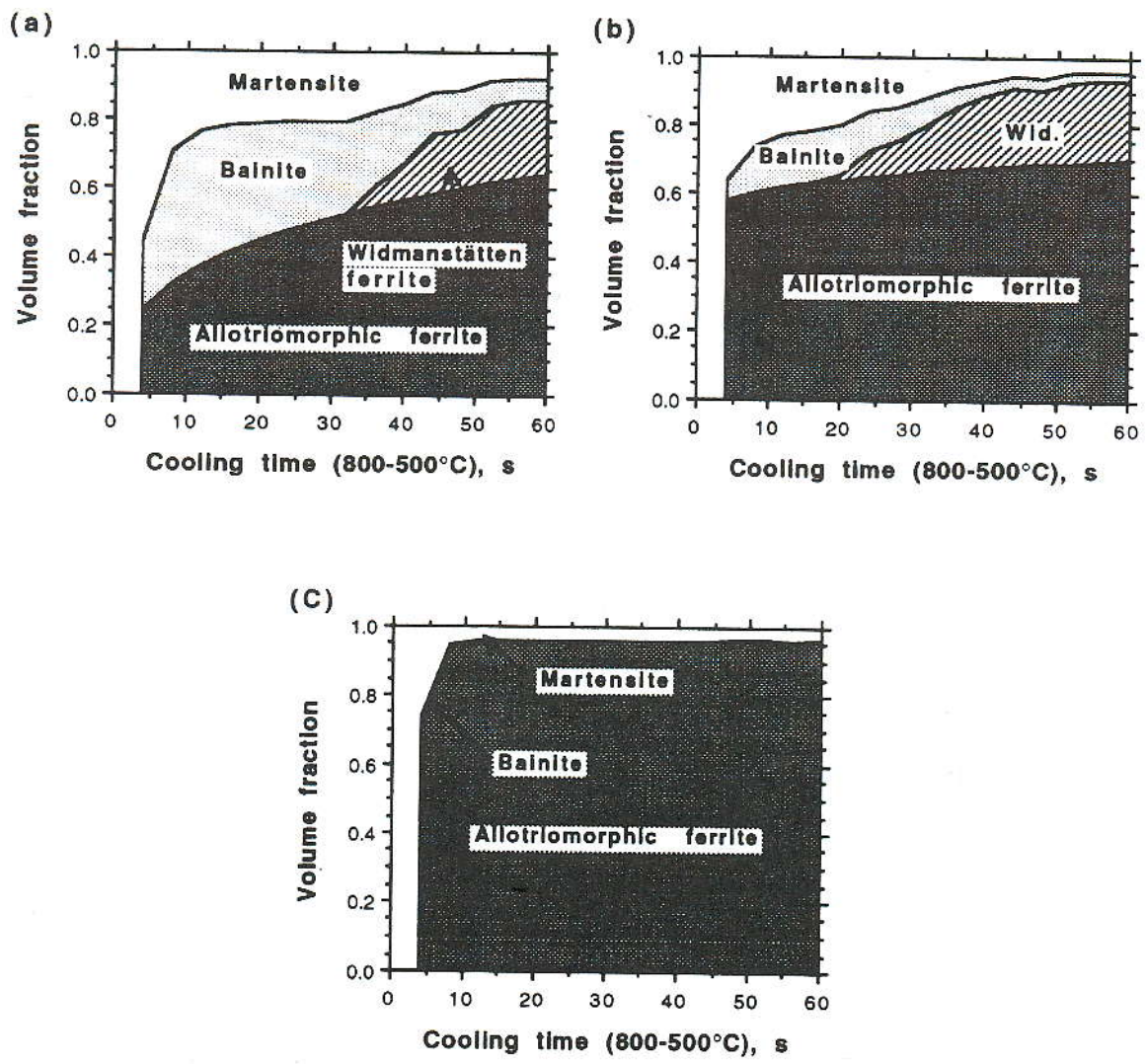


Figure 1: Fe-0.1C wt.% steel. (a) 100 μm austenite grain size, transformation from a fully austenitic sample. (b) 100 μm austenite grain size, transformation from a partially austenitic sample (0.5 volume fraction). (c) 30 μm austenite grain size, transformation from a fully austenitic sample.

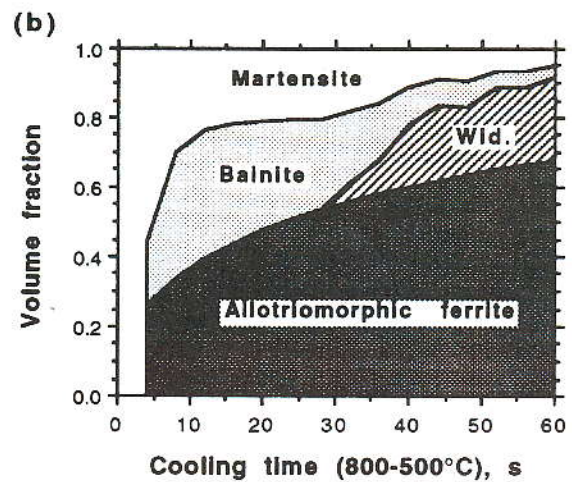
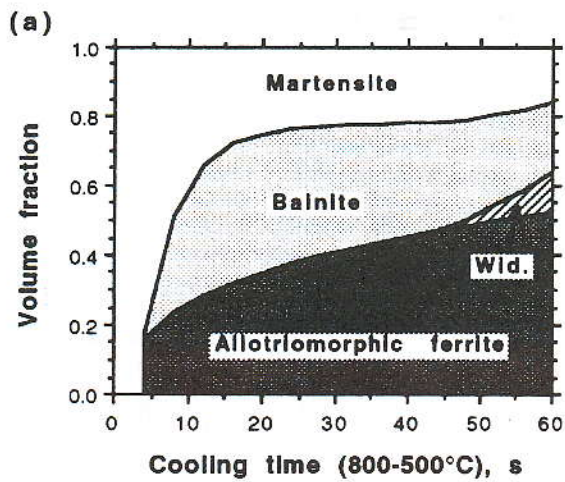


Figure 2: (a) Fe-0.1C-1.0Mn wt.% steel, 100 μm austenite grain size, transformation from a fully austenitic sample. (b) Fe-0.1C-1.0Si wt.% steel, 100 μm austenite grain size, transformation from a fully austenitic sample.

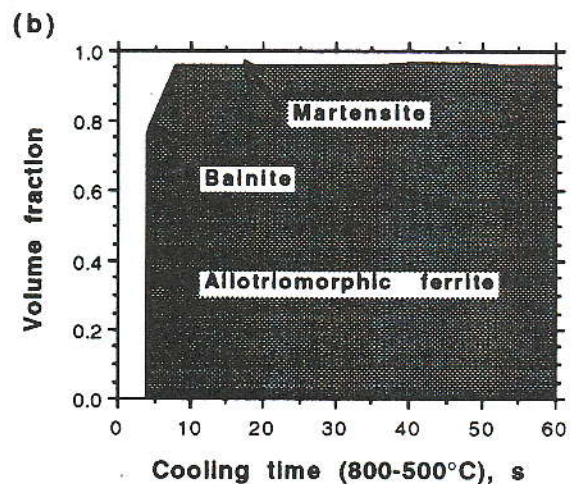
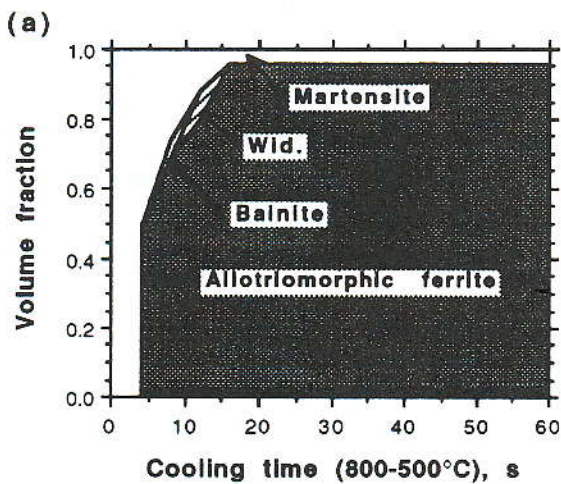


Figure 3: (a) Fe-0.1C-1.0Mn wt.% steel, 30 μm austenite grain size, transformation from a fully austenitic sample. (b) Fe-0.1C-1.0Si wt.% steel, 30 μm austenite grain size, transformation from a fully austenitic sample.